OncoTargets and Therapy

Dovepress
open access to scientific and medical research

Open Access Full Text Article

ORIGINAL RESEARCH

Inhibition of microRNA-126 promotes the expression of Spred1 to inhibit angiogenesis in hepatocellular carcinoma after transcatheter arterial chemoembolization: in vivo study

This article was published in the following Dove Press journal:
OncoTargets and Therapy
19 July 2016
Number of times this article has been viewed

Jian-Song Ji[1,2,*]
Min Xu[1,*]
Jing-Jing Song[1,*]
Zhong-Wei Zhao[1,*]
Min-Jiang Chen[1]
Wei-Qian Chen[1]
Jian-Fei Tu[1]
Xiao-Ming Yang[2]

[1]Department of Radiology, Affiliated Lishui Hospital of Zhejiang University, Fifth Affiliated Hospital of Wenzhou Medical University, Central Hospital of Zhejiang Lishui, Lishui, People's Republic of China; [2]Department of Radiology, Lab-Yang, University of Washington, Seattle, WA, USA

*These authors contributed equally to this work

Abstract: MicroRNA-126 (miR-126) has been found to promote angiogenesis, but the underlying mechanisms are still unclear. So, we conducted this study to explore the effect of miR-126 expression on angiogenesis in hepatocellular carcinoma (HCC) after transcatheter arterial chemoembolization (TACE). The expression levels of miR-126 and sprouty-related, EVH1 domain containing protein (Spred)1 in surgically resected HCC tissue, HCC tissue with TACE + operation, and tumor-adjacent tissues were determined by quantitative real-time polymerase chain reaction. The expression levels of miR-126, Spred1, and vascular endothelial growth factor were found by quantitative real-time polymerase chain reaction and Western blot. The microvessel density (MVD) of tumor tissues was determined by immunohistochemical staining. The miR-126 and Spred1 expressions in HCC tissue with TACE + operation were elevated and decreased, respectively, as compared to those in surgically resected HCC tissues and tumor-adjacent tissues (all $P<0.001$), which indicated that the expression of Spred1 was negatively correlated with miR-126 ($P<0.001$, $r=-0.6224$). Based on the bioinformatics analysis and luciferase reporter gene activity detection, Spred1 was found to target miR-126 ($P<0.001$). Inhibition of miR-126 expression reduces the degree of weight loss and tumor size in TACE model rats. The MVD in TACE + operation group was increased compared to that in the control group; inhibition of miR-126 expression had a reversal effect, to a certain extent, on MVD increase after TACE (all $P<0.05$). Inhibition of miR-126 expression increased Spred1 expression and decreased vascular endothelial growth factor expression ($P<0.01$). In summary, this study unveiled the potential mechanism by which miR-126 regulates angiogenesis in HCC tissues through embolization treatment by targeting Spred1, and also showed that the feasibility of TACE with the miR-126 inhibitor has a certain value in the medical treatment of HCC.

Keywords: microRNA-126, sprouty-related, EVH1 domain containing protein 1, hepatocellular carcinoma, transcatheter hepatic arterial chemoembolization, animal modeling, angiogenesis, vascular endothelial growth factor, microvessel density

Introduction

Hepatocellular carcinoma (HCC) is currently regarded as one of the most malignant cancers with a high incidence.[1] In the People's Republic of China, the annual HCC incidence is over 300,000, comprising 60% of the world's HCC incidence.[2] The current research suggested that the joint reactions between telomere shortening, chromosomal instability, and p21WAF1/CIP1 inactivation play important roles in HCC formation.[3] There are some histologic changes in this process, including changes

Correspondence: Xiao-Ming Yang
Department of Radiology, Lab-Yang, University of Washington, Box 358056, 815 Mercer Street, Room S470, Seattle 98109, WA, USA
Tel +1 206 685 6967
Fax +1 206 685 6967
Email y_xyxiao6309@163.com

submit your manuscript | www.dovepress.com
Dovepress
http://dx.doi.org/10.2147/OTT.S106513

in blood supply, material changes of water, fat, iron, and other components, and changes of cell nodules in shape, size, and density.[4] Surgical treatment is still an important means of HCC treatment. However, it has poor therapeutic effects and prognosis, mainly due to late diagnoses.[1] HCC is a typical multivessel tumor, and antiangiogenic therapy has become a research focus and an important method for HCC treatment.[5] Transcatheter arterial chemoembolization (TACE) therapy is a common nonsurgical antiangiogenesis treatment for HCC.[6]

MicroRNA (miRNA) is a noncoding, small-molecule RNA with a length of 20–24 nucleotides, which can match with its target genes in a 3′ noncoding region and inhibit the translation process of genes to accelerate its degradation.[7] A recent study has found that miRNA can regulate the development of multiple generations of tumors through the regulation of related genes' expression levels of cell proliferation and apoptosis.[8] Other studies have shown that there are some differentially expressed miRNAs in HCC tissues, which might be involved in a number of pathological processes on the generation, development, and metastasis of a tumor.[9–11] These studies also show that the miRNA abnormalities often exist before the occurrence of abnormal gene regulation. Therefore, adequate studies of different specific miRNA-targeting genes and their regulatory mechanisms can contribute to the diagnosis or treatment of HCC.[10,12] Evidence reported that sprouty-related, EVH1 domain containing protein (Spred) family members, including Spred1 and Spred2, had low expressions in tumor tissues, and were negatively correlated with tumor invasion and metastasis.[13] MicroRNA-126 (miR-126), the angiogenesis-related miRNA, is regarded as one of the main regulators of physiological angiogenesis.[14] Furthermore, miR-126 had impacts on vascularization of placenta, and had significant angiogenic effects both in ischemia-induced angiogenesis in vivo and cultured endothelial cells in vitro.[15,16] But some results of miRNA-related target site gene detection declared that miR-126 was one of the potential target genes of Spred1,[17] which has not yet been confirmed by other relevant studies. Therefore, this study was focused on verification of the target relationship between miR-126 and Spred1, as well as their related impacts on HCC angiogenesis after TACE.

Materials and methods

Ethical statement

This study was performed with the approval of experimental animal ethic committee of Wenzhou Medical University. Further, we conducted this experiment based on the welfare and ethical principles according to Welfare and Ethics of Medical Laboratory Animals. All the procedures involving subjects were performed in the study after obtaining the ethical approval of the Medical Ethics Committee of the University of Washington. All subjects provided written informed consent form.

Study subjects

HCC tissues that were preserved in the Department of Radiology, Lab-Yang, at the University of Washington from 2012 to 2015 were selected as study samples with complete clinical and pathological information. There were 70 HCC tissues from HCC patients who had undergone surgical resection after TACE (TACE + operation group), 70 surgically resected HCC tissues obtained by direct surgical resection (operation group), and 70 tumor-adjacent tissues (1 cm from the tumor) (control group). The hepatitis B surface antigen test results were recorded and the tumor node metastasis staging was implemented in accordance with the standards of the International Union Against Cancer,[18] and the Child–Pugh classification was applied according to the hepatic function.[19] The tissue samples were frozen in liquid nitrogen within 15 minutes and preserved at −80°C.

Luciferase reporter gene assay

Bioinformatics software from TargetScan and miTarget were used to detect target genes of miR-126. After the design and synthesis of reporter gene Spred1DNA fragments and Spred1DNA mutation fragments, the insertion of pGL4 luciferase vector (Promega Corporation, Fitchburg, WI, USA) was performed. HepG2 cells were purchased from Shanghai Cell Bank of Chinese Academy of Sciences (Shanghai, People's Republic of China). Cells were cultured in 5% CO_2 incubator at 37°C and subcultured every 3 days, and then were subjected to 0.25% trypsin digestion when cell attachment rate was up to 70%. According to the kit instructions of Dual-Luciferase Reporter Assay (Promega Corporation), the pGCsil-LV-miR126-GFP vector and the luciferase reporter gene vectors were cotransfected to HepG2 cells to form the miR-126 group; the pGCsil-LV-GFP blank vector and the luciferase reporter gene vectors were cotransfected to HepG2 cells to form the miR-negative control group (miR-NC group); the miR-126 inhibitors (Ribobio Biotechnology Company, Guangzhou, People's Republic of China) and the luciferase reporter gene vectors were cotransfected to HepG2 cells to form the miR-126-I group; the miR-126 inhibitors and the reporter gene mutation carriers were cotransfected to HepG2 cells to form the miR-126-IM group; the pGCsil-LV-miR126-GFP vectors and the reporter gene mutation

carriers were cotransfected to form the miR-126-M group; and the pGCsil-LV-GFP blank vector and the report gene mutation carriers were cotransfected to form the miR-NC-M group. Both miR-126 and miR-126 inhibitors share a common control sequence. Cells were lysed after 48 hours of being transfected and the lysate extraction was analyzed by a GloMax detection instrument (Promega Corporation).

HCC model establishment

Forty-eight healthy male Sprague-Dawley rats, aged 8 weeks and with body weight ranging from 175 to 220 g, were purchased from the Experimental Animal Center of Henan Province, License Number SCXK (Henan) 2005–2001. These rats were raised at 18°C–25°C. The healthy group consisted of 12 rats without any special treatment. Conventional culture of HepG2 cells was conducted, and cell suspension was prepared at a concentration of 1×10^7/mL. A cell suspension of 1 mL was extracted to be injected into the inside part of the hind leg of the remaining 36 Sprague-Dawley rats for subcutaneous tumor formation, which led to the formation of a palpable mass of size 1–2 cm after 2–3 weeks. The palpable tumor was removed under sterile conditions, and the tissue in the edge was cut into 1×1×1 mm grain sizes and reserved in Hanks' solution. The Sprague-Dawley rats were anesthetized by intraperitoneal injection of pentobarbital (50 mg/kg) and a 2.5 cm long incision was made on the midline of abdominal xiphoid under sterile conditions. Puncture of the liver capsule was made using ophthalmic scissors in the thicker parts of liver parenchyma on the outer left lobe (with a depth of approximately 0.5 cm), which was followed by application of tumor tablet implants and 2×2×2 mm-sized gelatin sponge to fill the wounds. The liver was reconstructed and the abdominal cavity sutured if there was no bleeding. A small animal magnetic resonance imaging (MRI) scans (ASPECT Imaging company, Modi'in, Israel) were conducted after 18 days after of implantation in order to calculate the HCC modeling rate of HepG2 on rats, observe the tumor intrahepatic growth, and measure the tumor diameter. A group of 36 successfully modeled rats were selected to perform TACE through hepatic artery gastroduodenal artery retrograde intubation. The control group (A) succeeded in hepatic artery gastroduodenal artery retrograde intubation and was injected with 0.2 mL of saline. The embolization group (B) underwent hepatic artery gastroduodenal artery retrograde intubation and was injected with 20 mg/kg of 5-fluorouracil and 0.4 mL/kg of lipiodol and saline suspension (lipiodol:saline =1:2). The embolization and miR-126 inhibiting group (C) underwent hepatic artery gastroduodenal artery retrograde intubation and was injected with 20 mg/kg of 5-Fu, 0.4 mL/kg of lipiodol and saline suspension (lipiodol:saline =1:2), and miR-126 inhibitor. There were 12 rats in each group, and the rats were euthanized within 21 days through an overdose of anesthetics. The non-necrosis tumor margin tissues were extracted as samples for subsequent experiments.

Quantitative real-time polymerase chain reaction detection of mRNA expressions of miR-126, Spred1, and vascular endothelial growth factor

Trizol reagent (Thermo Fisher Scientific, Waltham, MA, USA) was used to extract total RNA from the tissues according to the instructions. Then, the optical density (OD)260/280 values of the extracted RNA samples were measured with an ultraviolet spectrophotometer. The RNA concentration was calculated and the sample was preserved at 80°C for future use. Basic Local Alignment Search Tool (BLAST)-designed primers (synthesized by Thermo Fisher Scientific) were used, which are shown in Table 1. Experiments were carried out in accordance with the experimental procedure of the reverse transcription kit supplied by Takara Company (Tokyo, Japan). The Quantitative real-time polymerase chain reaction (qRT-PCR) method was applied with the PCR system from Beijing Transgen Biotech (Beijing, People's Republic of China). The PCR reaction system consisted of a total volume of 20 μL: 10 μL of 2× SYBR Green QPCR master mix, 0.3 μL of diluted reference dye, 0.2 μL of upstream primer (10 μmol/L), 0.2 μL of downstream primer (10 μmol/L), 0.3 μL of complementary DNA, and 0.9 μL of DEPC water. The reaction conditions were as follows: 10 minutes of denaturation at 95°C for one cycle, repeated for a total of 40 cycles, each with 30 seconds of denaturation at 95°C; 1 minute of annealing at 58°C; and 30 seconds of extension at 72°C. U6 was considered an internal control.

Table 1 Primer sequences

Name	Sequences
U6	For: 5′-CTCGCTTCGGCAGCACA-3′
	Rev: 5′-TGGTGTCGTGGAGTCG-3′
miR-126	For: 5′-TATAAGATCTGAGGATAGGTGG GTTCCCGAGAACT-3′
	Rev: 5′-ATATGAATTCTCTCAGGGCTAT GCCGCCTAAGTAC-3′
Spred1	For: 5′-GTCCTGCTGATGCTAGGGCT-3′
	Rev: 5′-GCCTGGCTGACCAAATGTTA-3′
VEGF	For: 5′-CGAAACCATGAACTTTCTGC-3′
	Rev: 5′-CCTCAGTGGGCACACACTCC-3′

Abbreviations: For, forward; miR-126, microRNA-126; Rev, reverse; Spred1, sprouty-related, EVH1 domain containing protein 1; VEGF, vascular endothelial growth factor.

The melting curve was applied to evaluate the reliability of PCR, and the average Ct value (amplified power curve inflection point) was chosen and used in semiquantitative analysis through $2^{-\Delta\Delta}$Ct to calculate the relative expression quantity of the target gene.

Western blot detection of the protein expression of Spred1 and vascular endothelial growth factor

Radioimmunoprecipitation assay was applied to extract the total protein in the tissues, the cell lysate of which was collected in an Eppendorf tube, followed by a 30 min ice bath and under a centrifugation of 12,000 rpm for 5 min at 4°C. The supernatant was transferred to another Eppendorf tube for BCA protein quantification and the precipitate discarded. After the protein extraction, a sample buffer was added to cook for 5 minutes at 95°C and the protein was separated through 10% volume of polyacrylamide gel electrophoresis with 30 μg for each protein sample. The electrophoresis was performed for 60 minutes; then 5% skim milk was added and preserved in phosphate-buffered saline (PBS) for 1 hour at room temperature, followed by the addition of Spred1 antibody (1:5,000), vascular endothelial growth factor (VEGF; 1:1,000), and β-actin antibody (1:1,000) purchased from Santa Cruz Biotechnology Inc. (Dallas, TX, USA) for overnight incubation at 4°C. Then, PBS equilibration was done for 1 hour at room temperature, followed by a PBS tween-20 (PBST) rinse (three times for 5 minutes). Appropriate secondary antibodies were added for incubation at room temperature for 1 hour and then washed with a membrane (three times for 5 minutes). Chemiluminescent reagents were used to develop the imaging. β-Actin was considered an internal control. Bio-rad Gel Doc EZ imager (Bio-Rad Laboratories Inc., Hercules, CA, USA) was used to develop the imaging. ImageJ software (National Institutes of Health, Bethesda, USA) was applied to analyze the gray value of the objective bands.

Immunohistochemistry detection of microvessel density counting

The immunohistochemical (IHC) staining method was used to calculate the microvessel density (MVD) values of tumor tissue for each group. The IHC staining and counting method was applied through CD34 antibody, which can label the endothelial cells and detect the MVD changes of tumor tissues. First, the full piece was viewed at low magnification (100×) of a light microscope to determine the area of highest vascular density. Second, five horizons of each slice were observed at high magnification (200×) of the light microscope to determine five values. The average value of the five visual fields was the MVD value. Individual endothelial cells or endothelial cell clusters were counted as a blood vessel, regardless of whether vessel lumen was there or not. The confusion or blur of stained cells and red blood cells with lumen area over the inner diameters of eight blood vessels were excluded.

IHC detection of protein expressions of Spred1 and VEGF

The specimens were fixed in 10% neutral buffered formalin and then embedded in paraffin. Primary antibodies were Spred1 monoclonal antibody (ab77079; Abcam Company, Cambridge, UK) and VEGF monoclonal antibody (ab1316; Abcam Company), respectively. SuperPicTure™ two-step method was used to detect Spred1 expression and IHC MaxVision™ method to detect VEGF expression, both dyed with diaminobenzidine. The specimens were subjected to a microwave antigen retrieval procedure in 0.01 mol/L sodium citrate buffer (pH 6.0) before IHC staining. The experiment was conducted according to the immunohistochemical Kit. Also, the positive slices of HCC incubated in PBS instead of the primary antibody were used as negative controls, and the positive slices of HCC were used as positive controls. Eight to ten horizons of each slice were observed at high magnification (×200) of the light microscope.

Statistical analysis

SPSS 22.0 software (IBM Corporation, Armonk, NY, USA) was applied to analyze the data and the measurement information was represented as (chi [χ] ±standard deviation). The *t*-test was used to compare the measurement data between two groups in accordance with normal distribution. One-way analysis of variance single-factor variance analysis was used to compare the counting data among multiple groups, and Pearson's method was used to carry out correlation analysis. The counting data were represented as percentage or rate, which were then subjected to χ^2 test. $P<0.05$ was considered statistically significant.

Results

General condition of subjects

Comparisons of sex, hepatitis B surface antigen, tumor diameter, number of tumors, tumor node metastasis staging, and liver function grading were made among HCC tissues in TACE + operation group and the operation surgery group (Table 2). There were no significant differences and the two sets of data were comparable (all $P>0.05$).

Table 2 Comparison of general conditions of patients in the operation group and the TACE + operation group (n=140)

Clinical information	Operation group (n=70)	TACE + operation group (n=70)	t	*P*-value
Sex				
Male	56	53	0.541	0.373
Female	14	17		
HBsAg				
+	65	63	0.365	0.546
–	5	7		
Diameter of tumors				
≥5 cm	48	45	0.288	0.591
<5 cm	22	25		
Number of tumors				
Single	53	49	0.578	0.447
Multiple	17	21		
TNM staging				
I	36	30	4.822	0.089
II	23	18		
III	11	22		
Liver function grading				
A	56	54	0.170	0.680
B	14	16		

Abbreviations: HBsAg, hepatitis B surface antigen; TACE, transcatheter arterial chemoembolization; TNM, tumor node metastasis.

Expression of miR-126 and Spred1 in various tissues

The results of qRT-PCR test showed that the miR-126 expression levels in HCC tissues in the TACE + operation group were significantly higher than those in the operation group, but lower than those in the tumor-adjacent tissue group (all $P<0.05$). The Spred1 expression level of HCC tissue in the TACE + operation group was significantly lower than that of the operation group, but higher than that of the tumor-adjacent tissue group (all $P<0.001$) (Figure 1). The correlation analysis showed that miR-126 was negatively correlated with Spred1 ($P<0.001$, $r=-0.6224$) (Figure 2).

Targeting relationship verification of miR-126 and Spred1

Bioinformatics analysis revealed that there was a complementary sequence between miR-126 and Spred1 in the untranslated regions region (Figure 3A). The results of

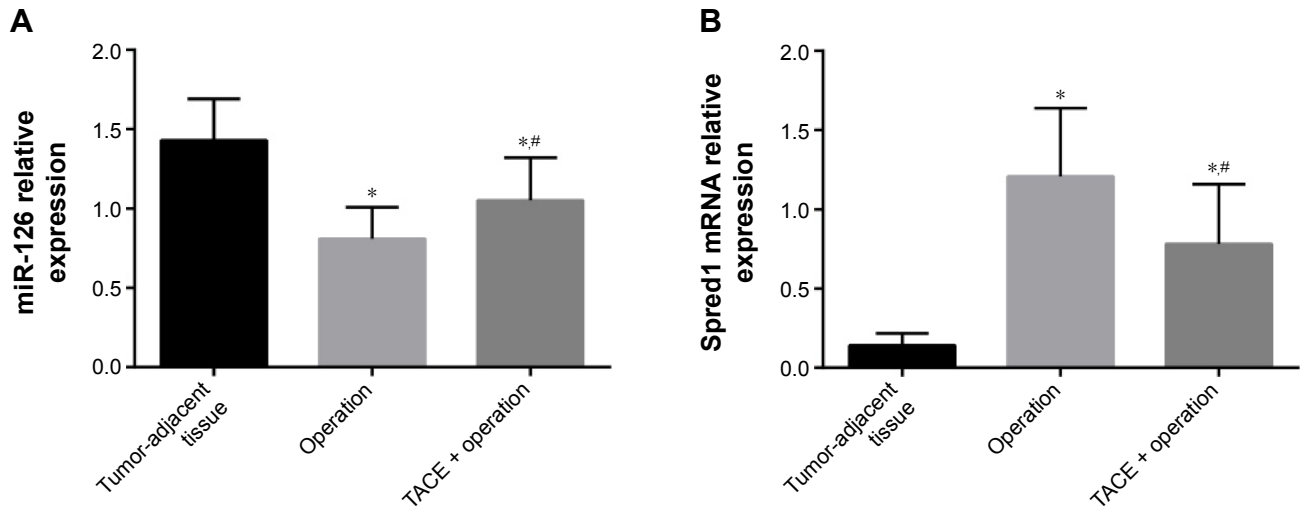

Figure 1 Expression of miR-126 and Spred1 in normal group, operation group, and TACE + operation group.
Notes: (**A**) Quantitative real-time polymerase chain reaction (qRT-PCR) detection of miR-126; (**B**) qRT-PCR detection of Spred1 mRNA. *Comparison with the normal group, $P<0.05$; #comparison with the operation group, $P<0.05$. Normal group: tumor-adjacent tissues.
Abbreviations: miR-126, microRNA-126; Spred1, sprouty-related, EVH1 domain containing protein 1; TACE, transcatheter arterial chemoembolization.

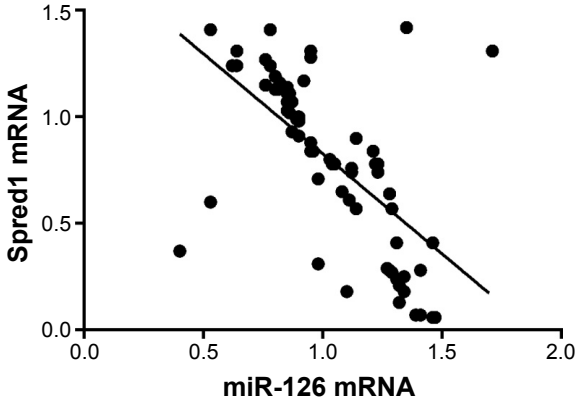

Figure 2 Correlation analysis of miR-126 and Spred1 mRNA expression for HCC patients in TACE + operation group.
Abbreviations: HCC, hepatocellular carcinoma; miR-126, microRNA-126; Spred1, sprouty-related, EVH1 domain containing protein 1; TACE, transcatheter arterial chemoembolization.

luciferase reporter gene assay showed that the Spred luciferase reporter gene activity of the miR-126 group decreased in comparison to that of the miR-NC group, but the luciferase reporter gene activity of miR-I, miR-126-M, miR-NC-M, and miR no-126-IM groups showed no obvious differences (Figure 3B).

General conditions of rats in each group

HepG2 liver tumors were successfully established in all 36 rats with 100% tumor formation rate and 100% survival rate. The MRI scan results showed that the tumor was on the left lobe of the liver with a relatively lower T_1WI signal and relatively higher T_2WI signal. The tumor size of T_1WI was 1.35±0.35 cm and that of T_2WI was 1.38±0.28 cm. The general conditions of the rats' weight and diet were observed after TACE and results showed that rats in the normal group had steady weight growth. All three groups of experimental rats experienced a loss in appetence within 3 days. Rats in group A began to recover within 3 days of surgery and rats in group C within 4 days of surgery, while rats in group B showed the worst appetence and began to recover within 5 days of surgery. Rats in each group showed decline in weight and appetence 14 days after surgery, wherein rats in group A were the worst, followed by rats in group B. Rats in group C showed relatively slow weight loss, which led to a statistically significant difference with the rats of group A within 21 days of surgery ($P<0.05$); there was no difference between group B and group C rats. The preoperative tumor sizes of each group were relatively the same, which was not statistically different. The results of tumor growth conditions detected by MRI scan on the 7th, 14th, and 21st days after surgery showed that the tumor size of groups B and C decreased gradually when compared to that of group A. The tumor size in group C was significantly smaller than in group B, indicating that the tumor growth was inhibited in group C ($P<0.05$) (Table 3; Figure 4).

Spred1 was a direct target of miR-126

MVD evaluation of the angiogenesis degree

The CD34 staining test results of MVD indicated that the MVD count of group B increased in comparison with that of group A, and the MVD count of group C decreased in

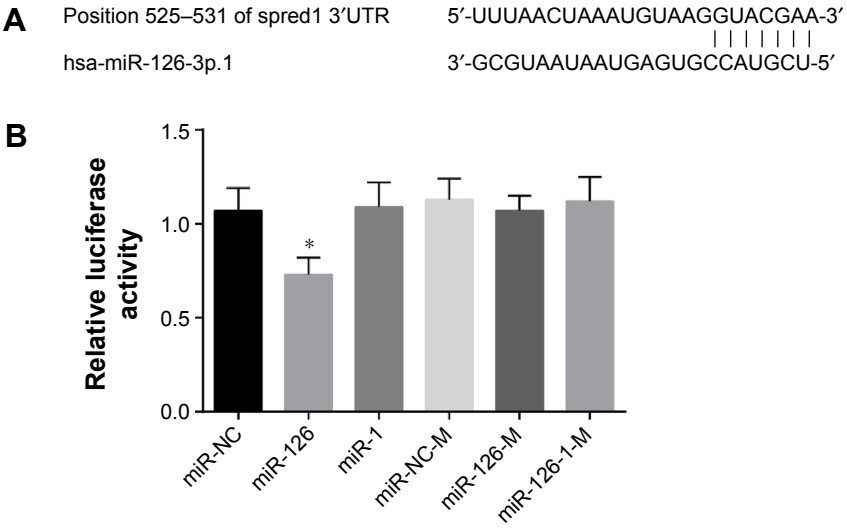

Figure 3 Targeting verification of miR-126 and Spred1 by bioinformatics analysis and Dual-Luciferase Reporter Assay.
Notes: (**A**) Sequence matches of Spred1 and miR-126. (**B**) The luciferase activity for each experimental treatment group. *Comparison to miR-NC group, $P<0.05$.
Abbreviations: miR-126, microRNA-126; NC, negative control; Spred1, sprouty-related, EVH1 domain containing protein 1.

Table 3 Pre- and postoperative changes in tumor size and weight

Group		Pre-operation	7 days after surgery	14 days after surgery	21 days after surgery
Normal group	Tumor size (cm^3)	0	0	0	0
	Weight (g)	255.72±13.60	270.55±12.98	287.14±14.24	298.83±13.03
A	Tumor size (cm^3)	1.79±0.18	1.81±0.15	1.98±0.16	2.15±0.22
	Weight (g)	252.26±10.39	262.57±12.72	269.35±14.02	273.74±15.24
B	Tumor size (cm^3)	1.81±0.23	1.77±0.17	1.70±0.10*	1.62±0.18*
	Weight (g)	254.63±15.37	265.36±13.34	273.57±16.83	280.32±16.77
C	Tumor size (cm^3)	1.82±0.14	1.75±0.21	1.61±0.19*	1.45±0.15*#
	Weight (g)	254.96±14.27	267.53±13.68	278.30±12.90	289.16±15.36*

Notes: *Comparison with group A, $P<0.01$; #comparison with group B, $P<0.05$. A, Control group; B, embolization group; C, embolization and miR-126 inhibiting group. Data are presented as mean ± standard deviation.
Abbreviation: miRNA, microRNA.

comparison with that of group B (all $P<0.05$) (Table 4; Figure 5).

mRNA and protein expression level changes of miR-126, Spred1, and vascular endothelial growth factor

The qRT-PCR test results showed that group B had the highest miR-126 expression levels, followed by group C and then group A (all $P<0.05$) (Figure 6), which indicated that the miR-126 inhibitors had successfully transfected the tumor tissue of the rats. The mRNA expression levels of Spred1 was the highest in group A, followed by group C and finally group B ($P<0.05$). The mRNA expression levels of VEGF were significantly increased in group A in comparison to those in group B ($P<0.001$). In comparison to group B, the mRNA expression levels of VEGF in group C were relatively lower, but still higher than those of group A ($P<0.05$). Western blot and IHC staining results revealed that the changes in Spred1 and VEGF protein levels were in accordance with the mRNA expression levels (Figures 7 and 8).

Discussion

In the present study, we aimed to explore the effect of miR-126 expression on angiogenesis in HCC patients after TACE. We first investigated the expression level of miR-126 and Spred1 in various tissues, including the HCC tissues from patients who were treated with TACE + operation and the tumor-adjacent tissues, and compared the differences in miR-126 and Spred1 expression in the patient clinical samples that involved TACE + operation and only operation, in order to explore the effects of miR-126 and Spred1 expression on angiogenesis in HCC after TACE. In order to better understand the alterations in expression levels and prognosis effect of miR-126 and Spred1 on angiogenesis in HCC after TACE, we established relevant rat models. The result of this study indicated that there was a significant reduction in tumor size and a gradual increase in weight of the experimental rats with a good prognosis after TACE, which could improve the efficacy of HCC treatment and reduce the occurrence of similar side effects in traditional chemotherapy. It has been reported that the differentiation of tumor blood vessels was uneven and they lacked muscular and sympathetic fibers. Chemoembolization can form a hypoxic environment inside the tumor, which accelerates the improvement of the suicide gene expression of VEGF promoters to achieve the killing effect.[20] Meanwhile, this kind of mediated embolization method can be applied with chemotherapy to make the chemotherapy drugs release slowly in the local tumor so that they can play a long-term role.

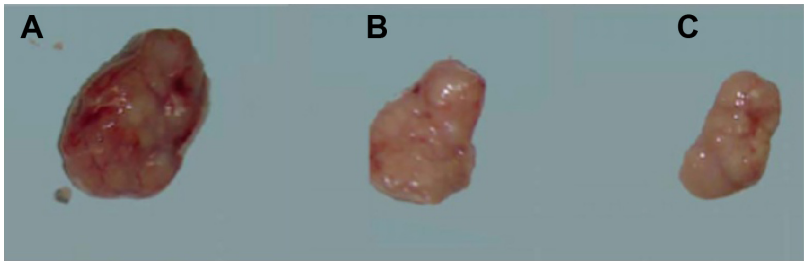

Figure 4 The tumor volumes of rats in each group 21 days after insertion, at which time they were injected with an overdose of anesthesia leading to death.
Notes: (**A**) Control group; (**B**) embolization group; (**C**) embolization and miR-126 inhibiting group.
Abbreviation: miR-126, microRNA-126.

Table 4 Comparison of the results of tumor tissue MVD count (N=10)

Group	MVD
A	31.87±3.51
B	69.56±4.85*
C	55.27±4.69*,#

Notes: *Comparison with group A, $P<0.05$; #comparison with group B, $P<0.01$. A, Control group; B, embolization group; C, embolization and miR-126 inhibiting group. Data are presented as mean ± standard deviation.
Abbreviations: miR-126, microRNA-126; MVD, microvessel density.

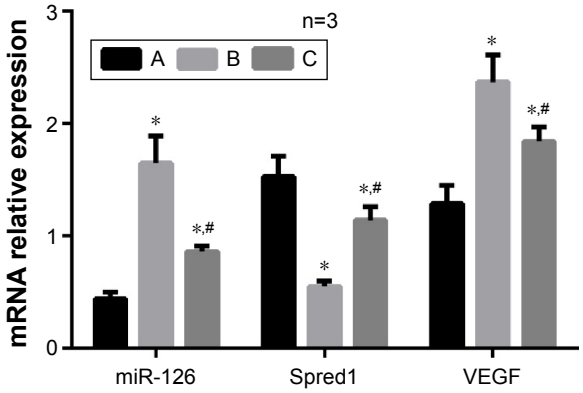

Figure 6 qRT-PCR detection of miR-126, Spred1, and VEGF expressions of tumor tissues in rats of each group.
Notes: *Comparison with group A, $P<0.05$; #comparison with group B, $P<0.05$. The variable n represents the repetition number of the experiment. A, Control group; B, embolization group; C, embolization and miR-126 inhibiting group.
Abbreviations: miR-126, microRNA-126; qRT-PCR, quantitative real-time polymerase chain reaction; Spred1, sprouty-related, EVH1 domain containing protein 1; VEGF, vascular endothelial growth factor.

On one hand, this study demonstrated that miR-126 targeted Spred1 and inhibited its expression level. Previous studies also showed that miR-126 and its complement miR-126* were encoded by epidermal growth factor-like domain 7, which, by repressing inhibitors of VEGF-induced proliferation in endothelial cells, could mediate blood vessel growth, integrity, and inflammation.[17,21,22] The miR-126 and epidermal growth factor-like domain 7 are highly expressed in endothelial cells.[23,24] Furthermore, Spred1 has been regarded as the target of miR-126 and by inhibiting Spred1, miR-126 can inhibit the VEGF pathway and, therefore, may promote angiogenesis.[17,25,26] The previous study reported that the expression level of Spred1 and the incidence rate of tumor invasion and metastasis were negatively correlated.[13] The correlated experiments in vitro and in vivo also showed that increase in the expression level of Spred1 can significantly inhibit tumor cells by decreasing the activity of ERK.[27,28] Meanwhile, high expression levels of Spred1 can inhibit the secretion of metalloproteinases MMP2 and MMP9, both of which play important roles in the processes of tumor invasion and metastasis.[29,30] Therefore, Spred1 can be considered a treatment site as well as a prognostic indicator. An increase in the expression levels of Spred1 can significantly inhibit the proliferation and invasion of HCC cells.[31]

On the other hand, the expression level of miR-126 significantly increased after TACE treatment. The results of such upregulated expression indicated that the increased expression was correlated with TACE treatment and, therefore, associated with the intracellular hypoxic–ischemic phenomenon caused by the treatment process of TACE.[32] In this situation, the high expression of miR-126 was also positively correlated with the level of VEGF, which suggested that there might be a defense mechanism for hepatoma cells regulated by miR-126, which accelerates blood transportation to reduce hypoxia through angiogenesis growth in order to resist the therapeutic effect of TACE. It has been reported that a single miRNA can modulate vascular function and

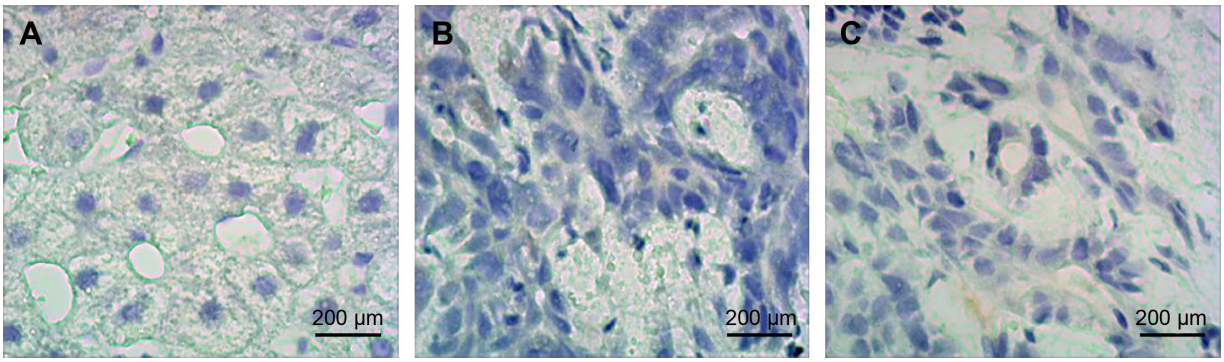

Figure 5 Immunohistochemistry determination of MVD for miR-126 targeting Spred1 in tumor tissues of rats in each group (light microscope, ×200).
Notes: (**A**) Control group; (**B**) embolization group; (**C**) embolization and miR-126 inhibiting group.
Abbreviations: miR-126, microRNA-126; MVD, microvessel density; Spred1, sprouty-related, EVH1 domain containing protein 1.

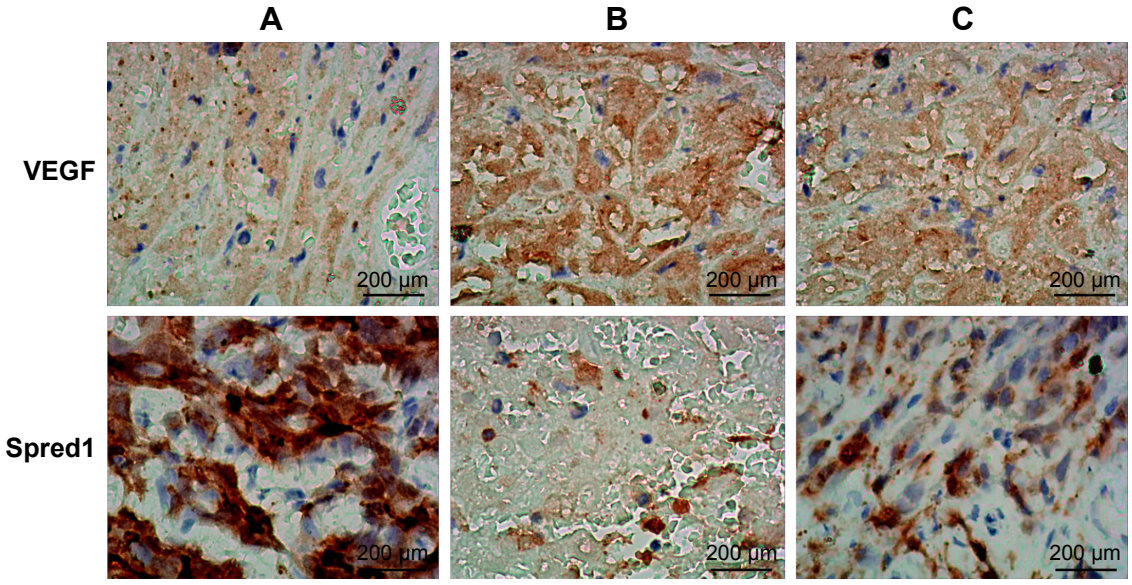

Figure 7 Immunohistochemistry detection of the protein expression of Spred1 and VEGF in tumor tissues in each group.
Notes: The positive expression of VEGF was defined as brown and brown-yellow stain, which was mainly located in the cytoplasm of cancer cells, and basically no positive expression of VEGF was found in stromal cells (×200). The positive expression of Spred1 was defined as brown-yellow in the cytoplasm of cancer cells, with yellowish brown stain in the cytoplasm, and basically no positive expression of Spred1 was found in stromal cells (×200). (**A**) Control group; (**B**) embolization group; (**C**) embolization and miR-126 inhibiting group.
Abbreviations: miR-126, microRNA-126; Spred1, sprouty-related, EVH1 domain containing protein 1; VEGF, vascular endothelial growth factor.

formation by regulating the vascular integrity and angiogenesis.[26] Previous studies showed that low expression of miR-126 in HCC was markedly related to tumor recurrence and can inhibit HCC cells' proliferation, invasion, and migration in vitro, which means that the downregulation of miR-126 is of great importance in HCC metastasis and has the advantages in prognosis prediction and HCC treatment.[33,34] Also, the antiangiogenic drugs probably can be used for TACE-treated HCC.[35] Therefore, the expression level of Spred1 can be restored to normal levels by inhibiting the expression levels of miR-126, which significantly increases the inhibition of the tumor proliferation and distinctively improves tumor prognosis.

This study demonstrated the relative evaluation and assessment of miR-126 with angiogenesis and prognosis effect through establishment of relevant rat models. However, further improvements are needed in some areas of this experiment. First, miR-126 may express differently in different types of cells; but in the present study, we failed to analyze the specific expression of miR-126 in different cell types. Moreover, the sample size of the experimental group was rather small, experimental funds were limited,

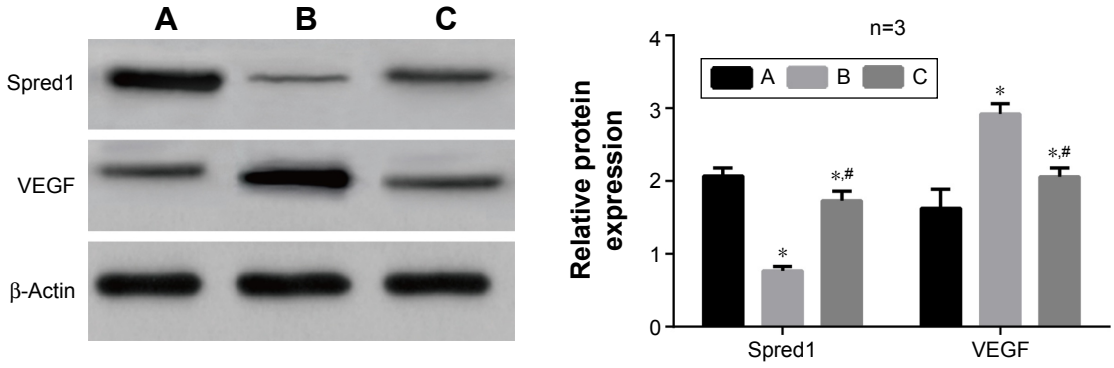

Figure 8 Western blot detection of the Spred1 and VEGF expressions of tumor tissues in each group.
Notes: *Comparison with group A, $P<0.05$; #comparison with group B, $P<0.05$. The variable n represents the repetition number of the experiment. **A**, Control group; **B**, embolization group; **C**, embolization and miR-126 inhibiting group.
Abbreviations: miR-126, microRNA-126; Spred1, sprouty-related, EVH1 domain containing protein 1; VEGF, vascular endothelial growth factor.

and experimental periods were not enough. Also, the side reflection, of the angiogenesis inhibition of miR-126 through the VEGF expression, was not sufficiently convincing.

In summary, this study demonstrated the mechanism by which miR-126 regulates angiogenesis in HCC tissues through embolization treatment, and also showed that the feasibility of TACE with miR-126 inhibitor has a certain value in the medical treatment of HCC.

Acknowledgments

This work was sponsored by Zheng Shu Medical Elite Scholarship Fund, the Major Social Development Program of Major Science and Technology Project of Zhejiang (Grant No 2013C03010), and the National Natural Science Foundation of China (81573657). We acknowledge the reviewers for their helpful comments on this paper.

Disclosure

Jian-Song Ji is working in the Fifth Affiliated Hospital of Wenzhou Medical University, which is also the Affiliated Lishui Hospital of Zhejiang University and is currently working on a postdoctoral degree in the University of Washington. The authors report no other conflicts of interest in this work.

References

1. Chen VL, Le AK, Kim NG, et al. Effects of cirrhosis on short- and long-term survival of patients with hepatitis B-related hepatocellular carcinoma. *Clin Gastroenterol Hepatol*. 2016;14(6):887–895.
2. Parkin DM, Bray F, Ferlay J, Pisani P. Global cancer statistics, 2002. *CA Cancer J Clin*. 2005;55(2):74–108.
3. Lee YH, Oh BK, Yoo JE, et al. Chromosomal instability, telomere shortening, and inactivation of p21(WAF1/CIP1) in dysplastic nodules of hepatitis B virus-associated multistep hepatocarcinogenesis. *Mod Pathol*. 2009;22(8):1121–1131.
4. Hu B, An HM, Wang SS, Chen JJ, Xu L. Preventive and therapeutic effects of chinese herbal compounds against hepatocellular carcinoma. *Molecules*. 2016;21(2):142.
5. Komatsu H, Iguchi T, Ueda M, et al. Clinical and biological significance of transcription termination factor, RNA polymerase I in human liver hepatocellular carcinoma. *Oncol Rep*. 2016;35(4):2073–2080.
6. Mukai Y, Wada H, Eguchi H, et al. [Complete surgical resection of a huge hepatocellular carcinoma invading the diaphragm and lung after transcatheter arterial chemoembolization (TACE) and sorafenib – a case report]. *Gan To Kagaku Ryoho*. 2015;42(12):1638–1640. Japanese.
7. Liu X, Tu J, Yuan J, et al. Identification and characterization of micrornas in snakehead fish cell line upon snakehead fish vesiculovirus infection. *Int J Mol Sci*. 2016;17(2).
8. Zhang B, Pan X, Anderson TA. MicroRNA: a new player in stem cells. *J Cell Physiol*. 2006;209(2):266–269.
9. Budhu A, Jia HL, Forgues M, et al. Identification of metastasis-related microRNAs in hepatocellular carcinoma. *Hepatology*. 2008;47(3):897–907.
10. Braconi C, Patel T. MicroRNA expression profiling: a molecular tool for defining the phenotype of hepatocellular tumors. *Hepatology*. 2008;47(6):1807–1809.
11. Ladeiro Y, Couchy G, Balabaud C, et al. MicroRNA profiling in hepatocellular tumors is associated with clinical features and oncogene/tumor suppressor gene mutations. *Hepatology*. 2008;47(6):1955–1963.
12. Wang L, Yue Y, Wang X, Jin H. Function and clinical potential of microRNAs in hepatocellular carcinoma. *Oncol Lett*. 2015;10(6):3345–3353.
13. Yoshida T, Hisamoto T, Akiba J, et al. Spreds, inhibitors of the Ras/ERK signal transduction, are dysregulated in human hepatocellular carcinoma and linked to the malignant phenotype of tumors. *Oncogene*. 2006;25(45):6056–6066.
14. Huang F, Zhu X, Hu XQ, et al. Mesenchymal stem cells modified with miR-126 release angiogenic factors and activate Notch ligand Delta-like-4, enhancing ischemic angiogenesis and cell survival. *Int J Mol Med*. 2013;31(2):484–492.
15. Yan T, Cui K, Huang X, et al. Assessment of therapeutic efficacy of miR-126 with contrast-enhanced ultrasound in preeclampsia rats. *Placenta*. 2014;35(1):23–29.
16. Yan T, Liu Y, Cui K, Hu B, Wang F, Zou L. MicroRNA-126 regulates EPCs function: Implications for a role of miR-126 in preeclampsia. *J Cell Biochem*. 2013;114(9):2148–2159.
17. Ishizaki T, Tamiya T, Taniguchi K, et al. miR126 positively regulates mast cell proliferation and cytokine production through suppressing spred1. *Genes Cells*. 2011;16(7):803–814.
18. Minagawa M, Ikai I, Matsuyama Y, Yamaoka Y, Makuuchi M. Staging of hepatocellular carcinoma: assessment of the Japanese TNM and AJCC/UICC TNM systems in a cohort of 13,772 patients in Japan. *Ann Surg*. 2007;245(6):909–922.
19. Ogasawara S, Chiba T, Ooka Y, et al. Sorafenib treatment in child-pugh a and b patients with advanced hepatocellular carcinoma: safety, efficacy and prognostic factors. *Invest New Drugs*. 2015;33(3):729–739.
20. Ovchinnikov RS, Mitrokhin VM, Mladenov MI. Effects of vascular endothelial growth factor-b on the bioelectric activity of rat atrial myocardium under normal conditions and during gradual stretching. *J Biol Regul Homeost Agents*. 2015;29(4):835–840.
21. Meister J, Schmidt MH. miR-126 and miR-126*: new players in cancer. *ScientificWorldJournal*. 2010;10:2090–2100.
22. Nikolic I, Plate KH, Schmidt MH. EGFL7 meets miRNA-126: an angiogenesis alliance. *J Angiogenes Res*. 2010;2(1):9.
23. Bai Y, Lu W, Han N, Bian H, Zhu M. Functions of miR126 and innate immune response. *Yi Chuan*. 2014;36(7):631–636.
24. Zhu N, Zhang D, Xie H, et al. Endothelial-specific intron-derived miR-126 is down-regulated in human breast cancer and targets both VEGFA and PIK3R2. *Mol Cell Biochem*. 2011;351(1–2):157–164.
25. DA Silva ND, Fernandes T, Soci UP, Monteiro AW, Phillips MI, DE Oliveira EM. Swimming training in rats increases cardiac micro RNA-126 expression and angiogenesis. *Med Sci Sports Exerc*. 2012;44(8):1453–1462.
26. Fish JE, Santoro MM, Morton SU, et al. Mir-126 regulates angiogenic signaling and vascular integrity. *Dev Cell*. 2008;15(2):272–284.
27. Kato R, Nonami A, Taketomi T, et al. Molecular cloning of mammalian Spred-3 which suppresses tyrosine kinase-mediated Erk activation. *Biochem Biophys Res Commun*. 2003;302(4):767–772.
28. Nobuhisa I, Kato R, Inoue H, et al. Spred-2 suppresses aorta-gonad-mesonephros hematopoiesis by inhibiting MAP kinase activation. *J Exp Med*. 2004;199(5):737–742.
29. Hennig M, Yip-Schneider MT, Wentz S, et al. Targeting mitogen-activated protein kinase kinase with the inhibitor PD0325901 decreases hepatocellular carcinoma growth in vitro and in mouse model systems. *Hepatology*. 2010;51(4):1218–1225.
30. Cruz-Muñoz W, Kim I, Khokha R. TIMP-3 deficiency in the host, but not in the tumor, enhances tumor growth and angiogenesis. *Oncogene*. 2006;25(4):650–655.
31. Momeny M, Khorramizadeh MR, Ghaffari SH, et al. Effects of silibinin on cell growth and invasive properties of a human hepatocellular carcinoma cell line, HepG-2, through inhibition of extracellular signal-regulated kinase 1/2 phosphorylation. *Eur J Pharmacol*. 2008;591(1–3):13–20.

32. Rong W, Yu W, Wu F, et al. [Effect of preoperative transcatheter arterial chemoembolization on the perioperative outcome of patients with hepatocellular carcinoma]. *Zhonghua Zhong Liu Za Zhi*. 2015; 37(9):671–675. Chinese.
33. Chen H, Miao R, Fan J, et al. Decreased expression of miR-126 correlates with metastatic recurrence of hepatocellular carcinoma. *Clin Exp Metastasis*. 2013;30(5):651–658.
34. He H, Huang Y, Yang D, et al. [Expression of miR-126/miR-126* in hepatocelluar carcinoma and its correlation with clinical outcomes]. *Nan Fang Yi Ke Da Xue Xue Bao*. 2014;34(10):1493–1497. Chinese.
35. Sergio A, Cristofori C, Cardin R, et al. Transcatheter arterial chemoembolization (TACE) in hepatocellular carcinoma (HCC): The role of angiogenesis and invasiveness. *Am J Gastroenterol*. 2008;103(4): 914–921.